

Modeling of temperature dependency of magnetization in straintronics memory devices

Mahmood Barangi and Pinaki Mazumder, *Fellow, IEEE*

Abstract— While a tremendous amount of work has been dedicated to the study of Langevin thermal noise field in spintronics magnetic tunneling junction (MTJ), a comprehensive model that predicts both static and dynamic responses of the magnetization due to temperature variations is yet to exist. In this work, we will first study the dependency of the saturation magnetization on temperature. We will then analyze the variations of the shape anisotropy and energy barrier of the straintronics MTJ on temperature. Lastly, we will incorporate these dependencies, along with the well-studied Langevin thermal field into the LLG equation to simulate the dynamic and static behavior of the straintronics devices.

I. INTRODUCTION

Aggressive scaling of CMOS technologies and the resulting increase in the leakage power and the energy densities have created a profusion of research interest in alternative technologies in order to find solutions that allows industry to keep up with the scaling pace predicted by Moore's Law [1]. Among the proposed technologies, spintronics memories and logic that operate based on the tunnel magnetoresistance (TMR) effect have attracted significant attention in the past years. Although TMR was discovered first in 1975 by Julliere [2], energy efficient methods to exploit this property in the ubiquitous integrated circuits were not present until the discovery of spin transfer torque effect (STT) [3]. STT demonstrates non-volatility, compatibility with CMOS circuitry, and performance and energy efficiencies that are almost comparable with the most efficient CMOS memories. However, due to the use of static currents, the STT's energy is yet far above the fundamental limits of the magnetic logic [4]. In order to remedy this and push the energy efficiency of the magnetic tunneling junction (MTJ), straintronics, as a voltage-based switching method, has been proposed recently [4-10].

Modeling of thermal noise by incorporating the Langevin field into the dynamic model of the spintronics devices has been studied comprehensively in recent years [11, 12]. It is demonstrated that the thermal noise has significant impacts on the flipping delay of the STT MTJ. Furthermore, as we will show in this paper, the straintronics MTJ, also has a strong dependency on the Langevin thermal noise field. Besides its direct influence on the initial angle of switching (and therefore, flipping delay) in MTJ, thermal noise affects the write error and hold error probabilities of the device.

M. Barangi is a graduate students research assistants at the department of EECS of the Univ. of Mich., Ann Arbor, MI 48109 USA (e-mail: barangi@umich.edu)

P. Mazumder is a professor with the department of EECS at the Univ. of Mich., Ann Arbor, MI 48109 USA (e-mail: mazum@eecs.umich.edu)

While the Langevin thermal field is used to predict the dynamic response of the device in the presence of thermal noise, the static properties and the energy barrier should also be studied in detail. The latter has important influences on the critical flipping voltage, initial magnetization angle, and data retention time. Analysis of both static and dynamic metrics of a straintronics device is the main goal of this work.

II. SATURATION MAGNETIZATION AND ENERGY BARRIER

Although the simplified model for the temperature dependency of the saturation magnetization, M_s , is given by the Bloch's Law [13], the method fails to predict the temperature dependencies at higher temperatures, while most of the integrated circuits (ICs) operate at temperature ranges between 200K and 400K. On the other hand, an alternative method based on the Brillouin function has proven to mimic the experimental data quite accurately [13]. The inaccuracy of the Bloch's model is emphasized in Fig 1 by comparing its data with the Brillouin data. The dependency of M_s on temperature is predicted by the Brillouin function as:

$$\frac{M_s(T)}{M_{s0}} = \frac{2J+1}{2J} \coth\left(\frac{2J+1}{2J}x\right) - \frac{1}{2J} \coth\left(\frac{1}{2J}x\right) \quad (1)$$

Where, J is the total angular momentum, and x , for a ferromagnetic material is given by:

$$x = \frac{M_{s0}(N_w\mu_0M_s(T))}{NkT} \quad (2)$$

Where, μ_0 is the permeability of vacuum, M_{s0} is the saturation magnetization at absolute zero, N_w is a material dependent constant, N is the number of atoms in the unit volume, and kT is the energy unit with k being the Boltzmann constant. By intersecting (1) and (2), the dependency of M_s on temperature can be obtained, which is plotted in Fig 2 for

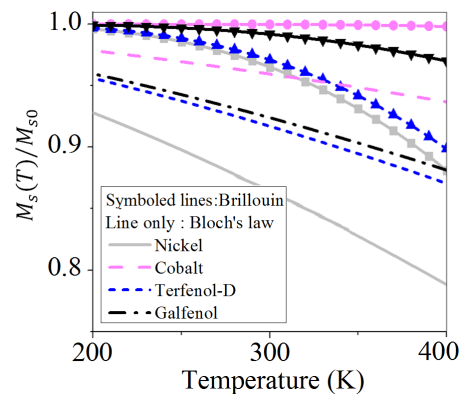


Fig 1. Bloch's law fails to predict the temperature dependency of M_s at higher temperatures

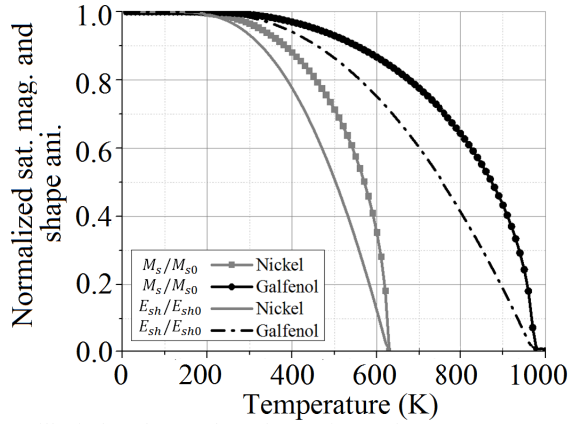


Fig 2. Brillouin-based temp. dependency of M_s and E_{sh}

Nickel and Galfenol. The resulting dependency of the shape anisotropy ($E_{sh} \propto M_s^2$ [4]) is also included in the graph.

A view of the straintronics device along with its electrical model is given in Fig 3. The energy barrier (EB) of the device, defined as the energy different between the hard axis and the easy axis of the MTJ, is a strong function of the applied stress [4]. When stress reaches a critical level, noted as σ_c , the energy barrier vanishes and the magnetization can freely rotate and settle along the minor axis, which is the basis of the straintronics switching. The dependency of the EB on temperature and the applied stress is further plotted in Fig 4. The strong dependency of EB on temperature emphasizes on the importance of static analysis of the temperature dependency along with the dynamic modeling.

The dependency of the shape anisotropy on temperature leads to the temperature dependency of the EB, as demonstrated in Fig 5. At temperatures close to absolute zero, due to the small value of T , the value of EB, measured in kT is very large. As the temperature approaches the Curie level, EB approaches zero, demonstrating a sharp drop in the logarithmic graph of the EB as a function of kT .

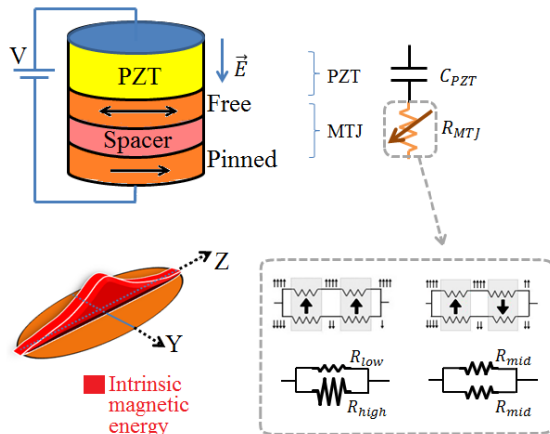


Fig 3. View of the straintronics device, demonstrating the energy barrier, the electrical model, and the resistance states of the MTJ; high resistance in antiparallel and low resistance in parallel orientations

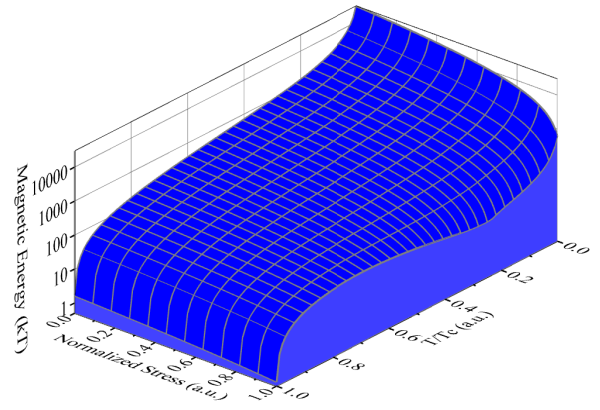


Fig 4. Temperature and stress dependency of Galfenol's energy barrier

III. SIMULATION RESULTS

While we used Brillouin function, discussed above, for modeling the static behavior of the straintronics device, the thermal noise, predicted by the Langevin distribution, needs to be included in the dynamic model to predict the effect of thermal fluctuations on the behavior of the nanomagnet. Conventionally, the dynamic behavior of the straintronics device's magnetization vector, \vec{M} , is modeled using the well-known Landau-Lifshitz-Gilbert (LLG) equation [4]:

$$\frac{d\vec{M}}{dt} = -\frac{\gamma_0}{(1+\alpha^2)}(\vec{M} \times \vec{H}) - \frac{\gamma_0}{M_s \times (\alpha + \frac{1}{\alpha})} \vec{M} \times (\vec{M} \times \vec{H}) \quad (3)$$

Here, α is the damping factor, γ_0 is the gyromagnetic ratio, and \vec{H} is the net magnetic field acting on the nanomagnet. The net magnetic field is mainly originating from the shape, uniaxial, and stress anisotropies. By simplifying (3) into the spherical coordinates, (r, θ, φ) , the instantaneous orientation of the magnetization vector, at any time, can be obtained using the following equations [4]:

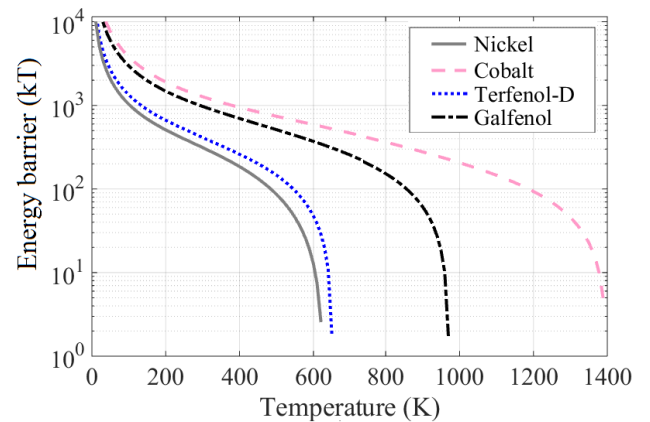


Fig 5. Temperature dependency of EB for different materials; as temperature approaches Curie levels, the energy barrier drops dramatically due to the strong reduction of the saturation magnetization

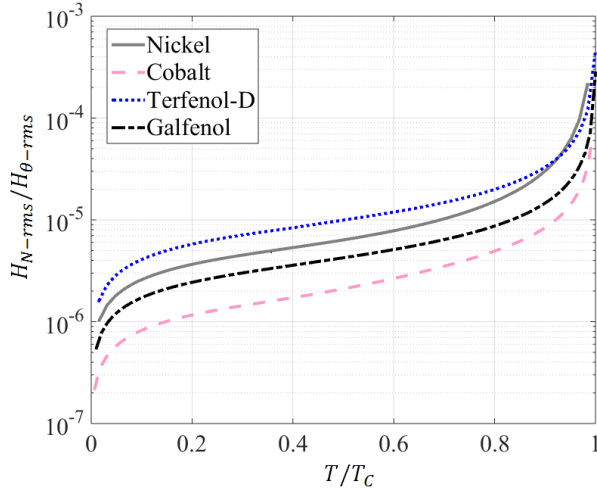


Fig 6. The relative strength of the thermal noise for different materials as a function of temperature; Cobalt's low damping factor contributes to its higher immunity against thermal noise

$$\frac{d\theta}{dt} = \frac{\gamma_0}{1 + \alpha^2} (H_\phi + \alpha H_\theta) \quad (4)$$

$$\frac{d\phi}{dt} = \frac{\gamma_0}{1 + \alpha^2} \frac{1}{\sin\theta} (\alpha H_\phi - H_\theta) \quad (5)$$

where, H_θ and H_ϕ are the spherical components of the net magnetic field in θ and ϕ directions, respectively.

The thermal noise can be modeled by incorporating the Langevin thermal field, H_N , into the LLG equation [11] and replacing the term H with $H_{tot} = H + H_N$, where:

$$H_{N,i} = \sqrt{\frac{2\alpha kT}{\mu_0 \gamma_0 M_s V}} X_i(t) \quad i = (x, y, z) \quad (6)$$

Here, V is the free layer's volume, and $X_i(t)$'s are uncorrelated zero-mean unit-variance Gaussian random variables in the direction of the Cartesian coordinates.

It would be worthwhile to investigate the effect of temperature and the choice of material on the relative strength

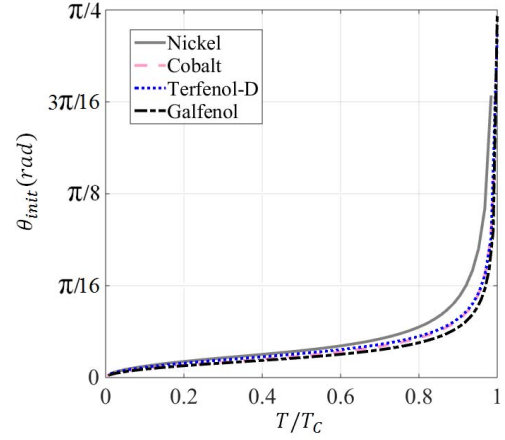


Fig 7. Initial magnetization angle as a function of temperature for different materials.

of the thermal noise, defined as H_N/H . The latter expresses the tendency of the magnetization vector to fluctuate around the major axis. The lower the relative strength is, the higher the fluctuations around the major axis will be. Fig 6 demonstrates the effect of temperature and choice of material on the relative strength of the thermal noise. At near-zero temperatures, (6) is very small, making the ratio negligible. As temperature rises, the thermal noise increases, while the net magnetic field due to magnetic energies becomes weaker mainly due to the reduction in the saturation magnetization. As temperatures get closer to the Curie level, the net magnetic field approaches zero, drastically increasing the relative strength of the thermal noise, as observed in the figure.

Incorporating the Langevin thermal noise field in the LLG equation leads to the fluctuations of the magnetization vector along the major axis in the absence of stress. The initial magnetization angle, θ_i , due to the thermal noise has a Gaussian variation with a root mean square (RMS) value of [14]:

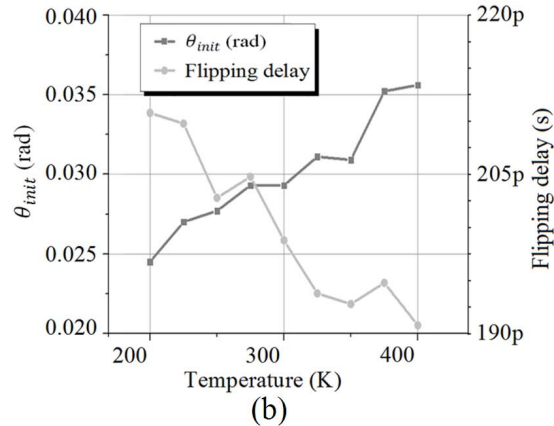
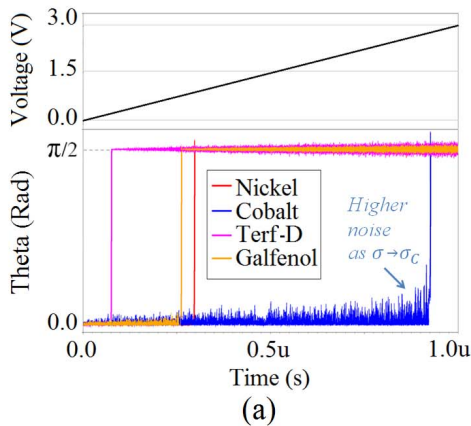


Fig 8. (a) Critical voltage of different materials; it is observed that as the ramp voltage approaches the critical stress, higher noise is observed, and (b) the dependency of the initial magnetization angle and flipping delay on temperature

$$\theta_{i-rms} = \sqrt{\frac{kT}{\mu_0 VM_s H}} \quad (7)$$

The variations of θ_i as a function of temperature is simulated and plotted in Fig 7. Nickel demonstrates higher fluctuations due to its lower M_s value, while Galfenol has the least fluctuation owing to its higher saturation magnetization. While a higher θ_i can essentially lead to a faster flipping, other material-dependent factors are also of crucial importance. For example, Galfenol, although demonstrating a lower magnetization fluctuation in (7), is considered a fast material for straintronics applications, mainly due to its high magnetostriction coefficient [4].

The simulation results on our model are demonstrated in Fig 8a for four different materials, where we applied a slow ramp across the straintronics device. As predicted by [4], Cobalt has the highest flipping delay due to its high M_s and low magnetostriction coefficient. It can be seen that as $\sigma \rightarrow \sigma_C$, the thermal noise becomes larger, which is due to the reduced energy barrier predicted in Fig 4.

Lastly, we simulated the effect of the temperature on the initial angle of the magnetization and its resulting impact on the flipping delay of the straintronics device in Fig 8b. As the temperature increases, the values of $H_{N,i}$ in (6) keep increasing. This leads to an increase in the initial magnetization angle as demonstrated in Fig 8b, and therefore, the critical flipping delay reduces, leading to a faster flipping of the magnetization vector.

IV. CONCLUSION

A comprehensive model for the straintronics MTJ was developed by incorporating both the Brillouin saturation magnetization and the Langevin thermal fields into the LLG equation. The analysis and methodology proposed in this work can be used for both straintronics and spintronics thermal modeling.

ACKNOWLEDGMENT

This work was done partially under NSF NEB grant ECCS-1124714 (PT106594-SC103006) and partially under AFOSR grant FA9550-12-1-0402.

REFERENCES

- [1] Moore, Gordon E., "Cramming more components onto integrated circuits, Reprinted from Electronics, volume 38, number 8, April 19, 1965, pp.114 ff.," *Solid-State Circuits Society Newsletter, IEEE*, vol.11, no.5, pp.33,35, Sept. 2006
- [2] Julliere, M. "Tunneling between ferromagnetic films," *Physics letters A*, vol. 54, no. 3, pp. 225-226, 1975
- [3] J. Slonczewski, "Current driven excitation of magnetic multilayers," *J. Magn. Magn. Mater.*, vol. 159, 1996
- [4] Barangi, M.; Mazumder, P., "Straintronics-based magnetic tunneling junction: Dynamic and static behavior analysis and material investigation," *Appl. Phys. Lett.*, vol.104, no.16, pp 162403, Apr 2014
- [5] Roy, K., Bandopadhyay, S. & Atulasimha, J., "Hybrid Spintronics and Straintronics: A magnetic technology for ultra-low energy computing and signal processing," *Appl. Phys. Lett.*, vol. 99, pp. 063108, 2011
- [6] Atulasimha, J. & Bandyopadhyay, S., "Bennett clocking of nanomagnetic logic using electrically induced rotation of magnetization

- in multiferroic single-domain nanomagnets," *Appl. Phys. Lett.*, vol. 97, pp. 173105, 2010
- [7] Kim, Sang-Koog; Shin, Sung-Chul; Kwangsoo No, "Voltage control of magnetization easy-axes: a potential candidate for spin switching in future ultrahigh-density nonvolatile magnetic random access memory," *Magnetics, IEEE Transactions on*, vol.40, no.4, pp.2637,2639, July 2004
- [8] N. Lei, T. Devolder, G. Angus, P. Aubert, L. Daniel, J. Kim, W. Zhao, T. Trypiniotis, R. P. Cowburn, C. Chappert, D. Ravelosona, and P. Lecoeur, "Strain-controlled magnetic domain wall propagation in hybrid piezoelectric/ferromagnetic structures," *Nature Communications*, vol. 4, Jan 2013
- [9] Khan, Asif; Nikonov, Dmitri E.; Maniaturuni, Sasikanth; Ghani, Tahir; Young, Ian A., "Voltage induced magnetostrictive switching of nanomagnets: Strain assisted strain transfer torque random access memory," *Applied Physics Letters*, vol.104, no.26, pp.262407,262407-5, Jun 2014
- [10] Barangi, M.; Mazumder, P., "Straintronics-Based Random Access Memory as Universal Data Storage Devices," *Magnetics, IEEE Transactions on*, vol.51, no.5, pp.1,8, May 2015
- [11] J. Z. Sun, et al, "Spin angular momentum transfer in a current-perpendicular spin valve nanomagnet," *Proceedings of SPIE*, vol. 5359, 2004
- [12] Nigam, A.; et al, "Delivering on the promise of universal memory for spin-transfer torque RAM (STT-RAM)," *ISLPED 2011*, vol., no., pp.121,126, 1-3 Aug. 2011
- [13] S. Chikazumi, "Physics of Ferromagnetism," Oxford University Press, Feb 1997
- [14] Maniaturuni, S.; Nikonov, D.E.; Young, I.A., "Modeling and Design of Spintronic Integrated Circuits," *Circuits and Systems I: Regular Papers, IEEE Transactions on*, vol.59, no.12, pp.2801,2814, Dec. 2012